

Decontamination of 2-chloroethyl ethylsulfide using titanate nanoscrolls

Alfred Kleinhammes^{a,*}, George W. Wagner^b, Harsha Kulkarni^a, Yuanyuan Jia^a,
Qi Zhang^a, Lu-Chang Qin^a, Yue Wu^a

^a Department of Physics and Astronomy and Curriculum in Applied and Materials Sciences, University of North Carolina at Chapel Hill, Chapel Hill, NC 27599-3255, United States

^b U.S. Army Edgewood Chemical Biological Center, Aberdeen Proving Ground, MD 21010-5424, United States

Received 15 February 2005; in final form 3 May 2005

Available online 24 June 2005

Abstract

Titanate nanoscrolls, a recently discovered variant of TiO₂ nanocrystals, are tested as reactive sorbent for chemical warfare agent (CWA) decontamination. The large surface area of the uncapped tubules provides the desired rapid absorption of the contaminant while water molecules, intrinsic constituents of titanate nanoscrolls, provide the necessary chemistry for hydrolytic reaction. In this study the decomposition of 2-chloroethyl ethylsulfide (CEES), a simulant for the CWA mustard, was monitored using ¹³C NMR. The NMR spectra reveal reaction products as expected from the hydrolysis of CEES. This demonstrates that titanate nanoscrolls could potentially be employed as a decontaminant for CWAs.

© 2005 Elsevier B.V. All rights reserved.

Hydrolysis reactions have shown promising reactivity and desirable products for the decontamination of a number of CWAs [1]. However, the solubility of some CWAs such as bis(2-chloroethyl) sulfide (HD or mustard) by aqueous solutions is often very limited, especially for thickened agents with added polymeric thickener [1]. This hinders severely the effectiveness of aqueous solutions for CWA decontamination [1]. An alternative approach to liquid decontamination media is the use of solid sorbent systems for the decontamination of CWAs and clean-up of hazardous waste pollutants [1]. Large surface area and sufficient reactivity toward pollutant detoxification are two key properties of the sorbent materials for such applications. Strong absorbance removes the agent rapidly from the affected surface and creates immediate relief. Once trapped with-

in the porous solid, the adsorbate undergoes chemical reactions which could render them harmless. The reaction chemistry involving detoxification of CWAs is shared by some organic pollutants and pesticides [1]. Recent experiments showed that powders of metal oxide, MgO [2], CaO [3], Al₂O₃ [4], and TiO₂ [5], when penetrated by CWAs, initiate reactions found in liquid decontamination schemes in addition to binding agents to their surfaces. Moreover catalysis was suspected as a means of sustaining some of the reactions [3]. It was expected that powders of nanocrystals would be more effective than powders of conventional microcrystals owing to larger surface areas and larger numbers of available reactive sites due to surface, corner, and edge defects [3,6]. In reality, much of that surface area would not be accessible to adsorbates due to aggregation of nanocrystallites rendering many facets of nanocrystallites inaccessible. In contrast to nanocrystals, nanostructures with large aspect ratios such as nanotubes and nanoscrolls might stack together irregularly without

* Corresponding author. Fax: +1 919 962 0480.

E-mail address: kleinham@physics.unc.edu (A. Kleinhammes).

loosing surface areas. One of such nanostructures is titanate nanoscrolls discovered in 1998 [7,8]. While the exact structure and composition are still under investigation, the dimension and shape as observed by TEM are clear [7–16]. The tubules have an average outer diameter of 12 nm and an inner diameter of 5 nm [10–12]. TEM characteristics such as a spiral-like cross-section reveal unambiguously the scroll structure (like a paper scroll). The spacing between the spiral walls of the nanoscroll is approximately 0.78 nm [10–12]. The uncapped tubules are on average between 0.3 and 1 μm long giving them large aspect ratio and large surface area. The surface area based on BET measurements is approximately 250 m^2/g for titanate nanoscrolls as compared to 50 m^2/g for typical TiO_2 nanocrystals [8]. Here, we demonstrate that titanate nanoscrolls have the potential to be an effective decontaminant for CWAs.

Titanate nanoscrolls were produced by hydrothermal synthesis following the procedure as originally proposed by Kasuga et al. [7,8] and followed by other authors [10–16]. 2 g of TiO_2 anatase nanocrystals (Aldrich 39953, 32 nm average particle size, 45 m^2/g surface area) was immersed in 200 ml of 10 M NaOH and heated in Teflon lined autoclave at 130 $^\circ\text{C}$ for 72 h. The produced material was sonicated, filtered, and washed repeatedly with distilled H_2O until the solution above the white precipitate becomes neutral (pH \sim 7). Dilute 0.1 M HCl was also used sometimes to speed up the process of reaching neutral pH. The precipitated material was then dried at temperatures around 55 $^\circ\text{C}$ for 3–5 h. The mass of the dried material exceeds the mass of the starting TiO_2 nanocrystals by a factor of approximately 1.6 indicating that the material contains H_2O molecules. The estimated ratio of H_2O to TiO_2 is about 3.5. ^{23}Na NMR was used to determine the Na content in the sample. The washed and dried nanoscrolls contain approximately 5×10^{20} Na/(g nanoscrolls) yielding a Na/Ti ratio of 0.07. This ratio is about 5 times higher in the sample immediately following the hydrothermal synthesis but without washing.

Pure 2-chloroethyl ethylsulfide (CEES) liquid, a simulant of HD, was used to evaluate the decontamination effect of titanate nanoscrolls. In the experiment, 3 μl of

pure CEES was added by a micro-syringe to 30 mg of titanate nanoscrolls (approximately 10 wt% CEES) packed in a magic-angle-spinning (MAS) rotor (4 mm MAS rotor from Chemagnetics/Varian). No additional water was added to the sample. The reaction path of CEES with titanate nanoscrolls was investigated by ^{13}C NMR. The CEES sample is not ^{13}C -enriched. Free induction decays (FIDs) were recorded using a pulsed spectrometer in a magnetic field of 9.4 T under MAS at a spinning rate of 10 kHz. The spectra were collected by signal averaging of 18 500 scans with a recycle delay of 5 s. Chemical shifts (CS) are reported with respect to TMS based on adamantane as a secondary reference.

Figs. 1a, b show scanning electron microscopy (SEM) pictures of our titanate nanoscrolls where the porosity of titanate nanoscroll aggregates is clearly revealed. Transmission electron microscopy (TEM) resolves the tubular structure with inner diameter of 5 nm and outer diameter of 12 nm (Fig. 1c). The wall separation is about 0.70 nm. Fig. 2 shows the X-ray diffraction (XRD) pattern (Cu $K\alpha$ line) of titanate nanoscroll powder. The prominent peak at $2\theta = 10.27^\circ$ was attributed to the separation of the walls of nanoscrolls and corresponds to a d-spacing of 0.86 nm. Suzuki and Yoshikawa [14] measured the d-spacing associated with this low angle diffraction peak as a function of temperature and found that d decreases from 0.92 nm at room temperature to 0.79 nm at 200 $^\circ\text{C}$. They attributed the observed change to water desorption from the space between the walls of nanoscrolls which deflate when water molecules are removed. Based on thermogravimetric measurements they estimated that nanoscrolls at room temperature contain $3\text{H}_2\text{O}$ per formula unit which they postulate to be $\text{H}_2\text{Ti}_3\text{O}_7 \cdot n\text{H}_2\text{O}$ with $n < 3$. Our nanoscrolls show a d-spacing of 0.86 nm as determined by XRD whereas TEM shows a d-spacing of 0.70 nm. Since TEM images were taken in ultrahigh vacuum and thus devoid of H_2O , the larger d-spacing determined by XRD is consistent with water trapping between the walls under ambient conditions. The relative change in the d-spacing is similar to that reported previously [14].

CEES ($\text{CH}_3\text{CH}_2\text{SCH}_2\text{CH}_2\text{Cl}$) and HD ($\text{ClCH}_2\text{CH}_2\text{SCH}_2\text{CH}_2\text{Cl}$) can be detoxified by stripping the chlorine

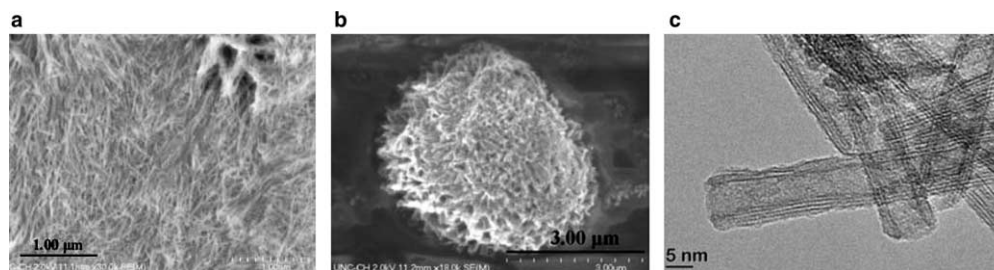


Fig. 1. SEM and TEM micrographs of titanate nanoscrolls. The images demonstrate the porosity of the material on length scales ranging from micro- to nanometers: (a) single particle, (b) surface of particle resembling a 'spider web' network of scrolls, (c) TEM image resolving individual nanoscroll.

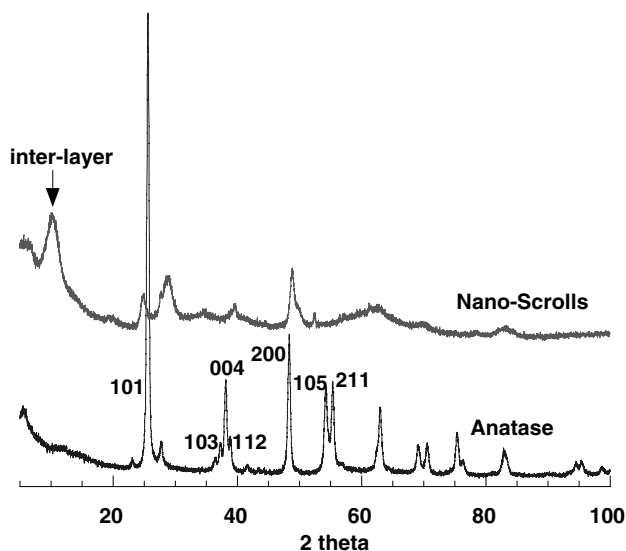


Fig. 2. X-ray diffraction pattern of titanate nanoscrolls. XRD pattern of anatase nanocrystals used in production of nanoscrolls is also shown for comparison. The prominent low angle peak associated with the interlayer spacing in nano-scrolls is indicated.

through hydrolysis to thiodiglycol ($\text{HOCH}_2\text{CH}_2\text{SCH}_2\text{-CH}_2\text{OH}$) [17] or be rendered non-vesicant by oxidation of the sulfur to form a sulfoxide ($\text{ClCH}_2\text{CH}_2\text{-S(=O)CH}_2\text{CH}_2\text{Cl}$) [18,19]. The reaction path of CEES during hydrolysis has been extensively studied [17]. A transient cyclic sulfonium cation– Cl^- anion pair shown schematically in Fig. 3a, too short-lived to be detected, is formed through intramolecular interaction of the sulfur

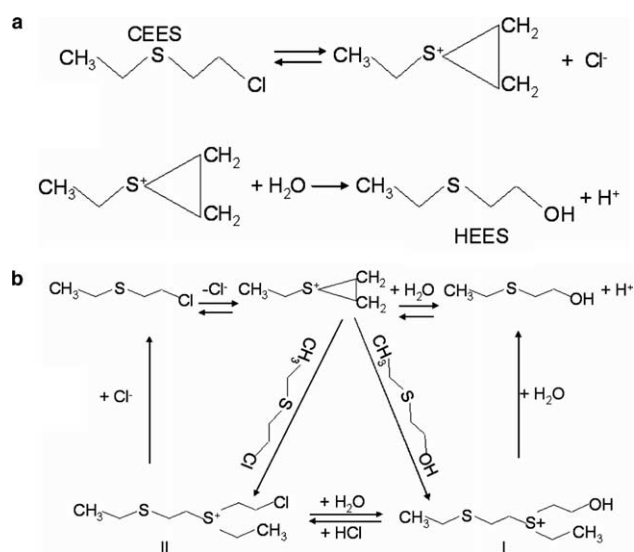


Fig. 3. (a) Reaction scheme for hydrolysis of CEES under low CEES concentration condition. The short-lived sulfonium cation– Cl^- anion pair is the intermediary between CEES and HEES. (b) Reaction scheme for hydrolysis of CEES under high CEES concentration condition. The dimeric cation II is formed predominantly at the early stage of the reaction. With declining CEES concentration, the reaction tilts toward the production of I which eventually converts to HEES.

on the chlorine. In low CEES concentration solutions the interaction of the sulfonium cation with H_2O dominates and produces 2-hydroxyethyl ethyl sulfide (HEES) and HCl (Fig. 3a). In solutions with larger concentrations of CEES ($\sim >0.1$ M) the reaction path is multi-branched (see Scheme I in [17] as reproduced in Fig. 3b) including the production of HEES ($\text{CH}_3\text{CH}_2\text{SCH}_2\text{CH}_2\text{OH}$) and two dimeric sulfonium cations I and II: I: $(\text{CH}_3\text{CH}_2\text{SCH}_2\text{CH}_2)\text{S}^+(\text{CH}_2\text{CH}_3)(\text{CH}_2\text{CH}_2\text{OH})$; II: $(\text{CH}_3\text{CH}_2\text{SCH}_2\text{CH}_2)\text{S}^+(\text{CH}_2\text{CH}_3)(\text{CH}_2\text{CH}_2\text{Cl})$. In hydrolysis the cation II is formed at the early stage of the reaction followed by conversion to cation I. The final products, after CEES and II being consumed, are HEES and cation I with I being the dominant species [17]. Over longer times (months) cation I converts to HEES with HEES becoming the most abundant and in the end final reaction product, unless a high HCl content forces an equilibrium between HEES and cation I [17].

The reaction products produced by the hydrolysis and oxidation of CEES were investigated previously by ^{13}C NMR [17,18,20]. Table 1 summarizes the ^{13}C chemical shifts of the hydrolysis reaction products of CEES based on previous studies. The ^{13}C chemical shifts of pure CEES determined by the present study (CS_{exp}) are also listed in Table 1. Fig. 4 shows the ^{13}C spectrum of pure liquid CEES. The triplets and quadruplet features are due to ^1H – ^{13}C exchange couplings of the ethyl and methyl groups. Also shown in Fig. 4 is the ^{13}C MAS spectrum taken 30 days after injecting CEES to titanate nanoscrolls packed in the MAS rotor. The chemical shifts of the various peaks identified as 1–7 are listed in Table 2 along with the integrated peak intensities (normalized to the intensity of peak 3). Comparing chemical shift values shown in Table 1, peak 1 at 9.8 ppm corresponds to either I'_1 or II'_1 and peak 7 at 61.6 ppm corresponds to H_4 . Possible assignments of the dominant line at 15.7 ppm (peak 2) are C_1 , H_1 , I_1 , II_1 . Possible assignments of the dominant line at 26.4 ppm (peak 3) are C_2 , H_2 , I_2 , I_3 , II_2 , II_3 . Final assignment of the spectral peaks is based on two observations. Peak C_4 is missing in the spectrum of CEES-injected titanate nanoscrolls, which is consistent with the scenario of complete conversion of CEES into HEES and I and/or II. The intensity ratio of peak 7 to peak 1 is about 1.4. Since peak 7 is exclusively associated with the hydroxy carbon (H_4) of HEES, it indicates that HEES is the dominant remaining reaction product. According to the reaction kinetics discussed above, HEES will only be the most abundant species if CEES and II are consumed and the conversion of I to HEES is the only active reaction. Therefore, peaks 1–7 are assigned to either HEES or I or both based on the chemical shift values as shown in Table 2. These assignments are in good agreement with the measured peak intensities. The expected peak intensities based on these

Table 1

Chemical formula and chemical shift (CS) of various compounds encountered in the hydrolysis reaction of CEES (CS with respect to TMS)

CEES	H ₃ C- (C ₁)	-CH ₂ -S- (C ₂)	-CH ₂ - (C ₃)	-CH ₂ - (C ₄)	-Cl					
CS [17]	17.1	28.1	36.1	46.4						
CS [20]	14.9	26.3	33.8	43.1						
CS _{exp}	15.9	27.0	34.6	44.1						
HEES	H ₃ C- (H ₁)	-CH ₂ -S- (H ₂)	-CH ₂ - (H ₃)	-CH ₂ - (H ₄)	-OH					
CS [17]	17.1	28.2	35.8	63.6						
CS [20]	14.9	25.6	34.8	60.5						
I	H ₃ C- (I ₁)	-CH ₂ -S- (I ₂)	-CH ₂ - (I ₃)	-CH ₂ - (I ₄)	-S ⁺ <	-CH ₂ - (I _{2'})	-CH ₃ (I _{1'})	-CH ₂ - (I ₅)	-CH ₂ - (I ₆)	-OH
CS [17]	16.7	28.2	28.2	42.9		37.5	11.2	45.2	59.0	
II	H ₃ C- (II ₁)	-CH ₂ -S- (II ₂)	-CH ₂ - (II ₃)	-CH ₂ - (II ₄)	-S ⁺ <	-CH ₂ - (II _{2'})	-CH ₃ (II _{1'})	-CH ₂ - (II ₅)	-CH ₂ - (II ₆)	-Cl
CS [17]	17.1	28.2	28.2	41.1		37.8	11.2	45.2	43.3	

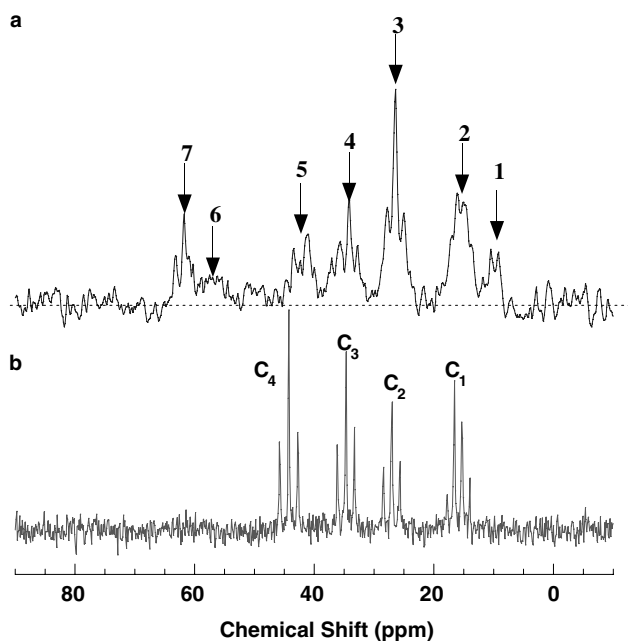
[] indicates the source of the CS data. CS_{exp} is from this work. CS values reported in [17] are systematically higher by about 2 ppm than other studies.

Fig. 4. ¹³C NMR spectra of: (a) liquid CEES, CH₃-CH₂-S-CH₂-CH₂-Cl (for the assignment of chemical-shift-resolved peaks C₁-C₄, see Table 1), (b) CEES injected to titanate nanoscrolls recorded 30 days after injection (for assignments of peaks 1-7, see Table 2).

assignments are listed in Table 2 along with the measured peak intensities. Another evidence for the absence of II is peak 6. Peak 6 at 57 ppm is consistent with I₆ but cannot be attributed to any carbon in II. Since the intensities of peak 6 and peak 1 are comparable, this suggests that peak 1 has to be associated predominantly with I. Thus, II has to be largely converted to I at this stage of the reaction. Notice that peak 6 at 57 ppm is quite broad compared to other peaks. This indicates that the OH⁻ group of I might interact strongly with the surface of titanate nanoscrolls. Another important issue related to the development of decontaminants is the reaction rate. Since natural ¹³C abundance CEES was used here, it is not practical to measure this at the moment. NMR can be used to measure quantitatively the reaction rate using ¹³C-enriched CEES and CWAs [2-4]. This approach is currently being used to investigate the reaction rates of CWAs with titanate nanoscrolls. Preliminary results [21] show that titanate nanoscrolls indeed compare favorably with existing solid decontaminant systems such as Al₂O₃ nanoparticles.

In summary, the described experiment showed that titanate nanoscrolls are well suited for the decontamination of CWA HD. The tubules offer large surface area

Table 2

Peak labels of the ¹³C MAS spectrum in Fig. 4, the corresponding CS values, measured peak intensities normalized to peak 3 intensity, possible peak assignments based on CS values, the final assignments (see discussion in the text), and expected peak intensities based on the final assignments

Peak labels	CS (ppm)	Normalized peak intensities	Possible assignments	Final assignments	Expected peak intensities
1	9.8	0.3	I _{1'} , II _{1'}	I ₁	0.3
2	15.7	0.8	C ₁ , H ₁ , I ₁ , II ₁	H ₁ , I ₁	0.7
3	26.4	1.0	C ₂ , H ₂ , I ₂ , I ₃ , II ₂ , II ₃	H ₂ , I ₂ , I ₃	1
4	34.1	0.7	I _{2'} , C ₃ , H ₃	I _{2'} , H ₃	0.7
5	42	0.5	I ₄ , I ₅ , II ₄ , II ₅ , II ₆	I ₄ and I ₅	0.6
6	57.0	0.3	I ₆	I ₆	0.3
7	61.6	0.4	H ₄	H ₄	0.4

and sufficient chemical reactivity to quickly absorb the agent, encapsulate it, and render it harmless through hydrolysis chemical reactions. No external water needs to be added for the hydrolysis reaction other than the intrinsically contained water in titanate nanoscrolls. The use of titanate nanoscrolls as decontaminants offers an environmentally friendly approach to hazardous material clean-up. TiO_2 is known as a photocatalyst [22] and titanate nanoscrolls could have similar photocatalytic properties. In future studies this aspect of the decontamination scheme will be investigated.

Acknowledgments

We thank Adam Hall for his help in obtaining SEM images and Thomas Sünner and James Spence for their assistance in sample preparation. This work was supported by ARO under contract DAAD19-03-1-0326 and by NSF under contract DMR-0139452.

Appendix A. Supplementary data

Supplementary data associated with this article can be found, in the online version, at [doi:10.1016/j.cplett.2005.05.100](https://doi.org/10.1016/j.cplett.2005.05.100).

References

- [1] Y.-C. Yang, J.A. Baker, J.R. Ward, *Chem. Rev.* 92 (1992) 1729.
- [2] G.W. Wagner, P.W. Bartam, O. Koper, K.J. Klabunde, *J. Phys. Chem. B* 103 (1999) 3225.
- [3] G.W. Wagner, O.B. Koper, E. Lucas, S. Decker, K.J. Klabunde, *J. Phys. Chem. B* 104 (2000) 5118.
- [4] G.W. Wagner, L.R. Procell, R.J. O'Connor, S. Munavalli, C.L. Carnes, P.N. Kapoor, K.J. Klabunde, *J. Am. Chem. Soc.* 123 (2001) 1636.
- [5] G.W. Wagner, L.R. Procell, S. Munavalli, private communications.
- [6] K.J. Klabunde, J. Stark, O. Koper, C. Mohs, D.G. Park, S. Decker, Y. Jiang, I. Lagadic, D. Zhang, *J. Phys. Chem.* 100 (1996) 12142.
- [7] T. Kasuga, M. Hiramatsu, A. Hoson, T. Sekino, K. Niihara, *Langmuir* 14 (1998) 3160.
- [8] T. Kasuga, M. Hiramatsu, A. Hoson, T. Sekina, K. Niihara, *Adv. Mater.* 11 (1999) 1307.
- [9] W. Wang, O.K. Varghese, M. Paulose, C.A. Grimes, Q. Wang, E.C. Dickey, *J. Mater. Res.* 19 (2004) 417.
- [10] Q. Chen, G.H. Du, S. Zhang, L.-M. Peng, *Acta Cryst. B* 58 (2002) 587.
- [11] S. Zhang, L.-M. Peng, Q. Chen, G.H. Du, G. Dawson, W.Z. Zhou, *Phys. Rev. Lett.* 91 (2003) 256103.
- [12] G.H. Du, Q. Chen, R.C. Che, Z.Y. Yuan, L.-M. Peng, *Appl. Phys. Lett.* 79 (2001) 3702.
- [13] R. Ma, Y. Bando, T. Sasaki, *Chem. Phys. Lett.* 380 (2003) 577.
- [14] Y. Suzuki, S. Yoshikawa, *J. Mater. Res.* 19 (2004) 982.
- [15] X. Sun, Y. Li, *Chem. Eur. J.* 9 (2003) 229.
- [16] B.D. Yao, Y.F. Chan, X.Y. Zhang, W.F. Zhang, Z.Y. Yang, N. Wang, *Appl. Phys. Lett.* 82 (2003) 281.
- [17] Y.-C. Yang, L.L. Szafraniec, W.T. Beaudry, J.R. Wagner, *J. Org. Chem.* 53 (1988) 3293.
- [18] Y.-C. Yang, L.L. Szafraniec, W.T. Beaudry, *J. Org. Chem.* 55 (1990) 3664.
- [19] G.W. Wagner, L.R. Procell, Y.-C. Yang, C.A. Bunton, *Langmuir* 17 (2001) 4809.
- [20] C.J. Pouchert, J. Behnke (Eds.), *The Aldrich Library of ^{13}C and ^1H FT NMR Spectra*, edn. I, Milwaukee, 1993.
- [21] G.W. Wagner, A. Kleinhammes, Harsha Kulkarni, Yue Wu, unpublished results.
- [22] J. Borisch, S. Pilkenton, M.L. Miller, D. Raftery, J.S. Francisco, *J. Phys. Chem. B* 108 (2004) 5640.